Available online at www.sciencedirect.com

ScienceDirect

Procedia Engineering 63 (2013) 36 – 44

Procedia Engineering

www.elsevier.com/locate/procedia

The Manufacturing Engineering Society International Conference, MESIC 2013

# Cutting conditions and surface integrity during dry plunge-milling of a wrought magnesium alloy

I. Danis[a,*], N. Wojtowicz[b], F. Monies[a], P. Lamesle[c], P.Lagarrigue[d]

[a]*Université de Toulouse UPS, Institut Clément Ader (ICA), 118 route de Narbonne 31062 Toulouse cedex 9, France*
[b]*Université de Toulouse ISAE, ICA, 10 avenue E. Belin, BP 54032, 31055 Toulouse, France*
[c]*Université de Toulouse EMAC, ICA, Campus Jarlard 81013 Albi cedex 9, France*
[d]*Université de Toulouse ISAE JFC, ICA, Place de Verdun, 81012 Albi cedex 9, France*

**Abstract**

Plunge milling is a machining process used to remove material rapidly in roughing operations. It is known to offer significant increases in productivity as compared with conventional milling, especially in the case of deep milled workpieces. However, high productivity also entails the increase in machining conditions so it would be expected that plunge milling has more impact on surface integrity than conventional machining. In this study the authors consider the case of a dry plunge milling process applied to a wrought Mg-Zr-Zn-RE alloy. First, the study involves obtaining surfaces through experimental design. Second, plunge milling conditions are correlated with surface integrity factors, such as roughness, microstructure and microhardness. This study suggests plunge milling conditions to offer a trade-off between surface integrity and chip flow.



*Keywords:* Plunge-milling; dry machining; magnesium alloy; surface integrity

## 1. Introduction

Plunge-milling is a machining process used to remove material rapidly during roughing operations. It can be used to achieve major increases in productivity, especially in the case of deep milled workpieces. The authors of

* Corresponding author. Tel.: +3-356-155-8176; fax: +3-356-155-8178.
*E-mail address:* danis@lgmt.ups-tlse.fr


doi:10.1016/j.proeng.2013.08.213

the present article are involved in the CARAIBE project, one of whose goals is to reduce manufacturing costs for a machined engine housing made of a wrought magnesium alloy. Reducing costs means increasing chip flow, preferably without any lubrication and especially during roughing operations. This explains why the authors chose to study plunge-milling, especially as the engine housing tolerances allow some scallop height (Fig. 2) so that finishing operations can be avoided. However, this improvement of productivity could be harmful to surface integrity.

Various issues of plunge-milling have already been covered, like chatter stability (Altintas and Ko), cutting tool geometries (Witty et al.) or accuracy of vertical walls (Wakaoka et al.), but none of them deals with the effect of plunge-milling on surface integrity. Moreover, the said studies were not performed on magnesium alloys, but on aluminium alloys (Altintas and Ko), steel X3CrNiMo13-4 (Witty et al.), grey cast iron or plain carbon steel (Wakaoka et al.). Surface integrity during machining of magnesium alloys was studied by Pu et al, and Salahshoor and Guo. Indeed, Pu observed dry and cryogenic orthogonal cutting of an AZ31 magnesium alloy: decreasing temperature led to a minor FBU formation and a better surface roughness. On the surface, the grains were oriented in cutting direction, and their size changed to nano-scale. Salahshoor and Guo studied high-speed dry milling of magnesium-calcium alloy for orthopaedic applications. Contrary to Pu et al, no grain refinement or orientation was observed, as the large grains were cut through. In both cases, the materials showed more important hardness and highly compressive residual stress on surface.

To the authors' knowledge, no work has been done on the influence of plunge-milling conditions on surface integrity of a magnesium alloy. The authors will thus be in a position to offer a trade-off between chip flow and surface integrity of a wrought Mg-Zr-Zn-RE alloy.

## 2. Methodology and experimental procedure

The machined material was Elektron 21 alloy (Lyon et al., Kielbus), as marketed by Magnesium Elektron before being forged in France. It was received in the form of 800 mm long bars with a rectangular cross-section of 100 mm x 150 mm. These bars were then cut off every 100 mm to provide the test coupons. The plunge cuts were always made in the lengthwise direction of the bar (Fig. 1).

The plunge milling tests were performed on a DMU eVolution 5-axis NC machine (Siemens 840D), without lubrication. The test coupons were secured to a Kistler six-component force measurement plate 9257B. The cutting tool used was a 33 mm diameter Mitsubishi AQX milling cutter. Only a single insert (grade HTi10 for non-ferrous alloys) was mounted so as to facilitate study of cutting while avoiding axial or radial run-out, as well as the overlapping of loads due to each tooth. Some tests were filmed using a high-speed camera so as to monitor vibration phenomena.

The tests involved performing successive plunge cuts into a test coupon, each time shifting by a radial offset value noted ae (Fig. 2). The cutting conditions were modified on each descent of the cutter into the material, in accordance with a design of experiments where 3 two-levels input parameters were subject to variation: ae, the feed fz and the cutting speed Vc. The design of experiments bounds are shown in table 1. Eight tests were performed at the limits of the domain; three additional tests at intermediate values of Vc and fz, and three tests at lower Vc were performed in order to complete this methodology. Due to confidential issues, the values for Vc and fz are not given. They are stated as a percentage of the cutting conditions Vc* and f* given by Mitsubishi for this tool in aluminium alloys. The radial depth of cut ae is chosen so that the scallop height (h) (Fig. 2) does not exceed 0.3 mm.

Table 1. Variation ranges of cutting conditions.

| | |
|---|---|
| Cutting speed Vc | Vcmin=80% of Vc* to Vcmax=200% of Vc* |
| Feed per tooth fz | fzmin=154% of f* to fzmax=1846% of f* |
| Radial offset $a_e$ | ae1 and ae2 (ae2=2.ae1), with h<0.3 mm |

For each cutting condition, the surface resulting from the entry of the cutter into the material as well as that created by its exit can thus be studied (Fig. 1 and 3). When plunge milling a pocket or a housing, the walls will

indeed result either from the cutter entry or the cutter exit, except in the angles where a greater surface is conserved.

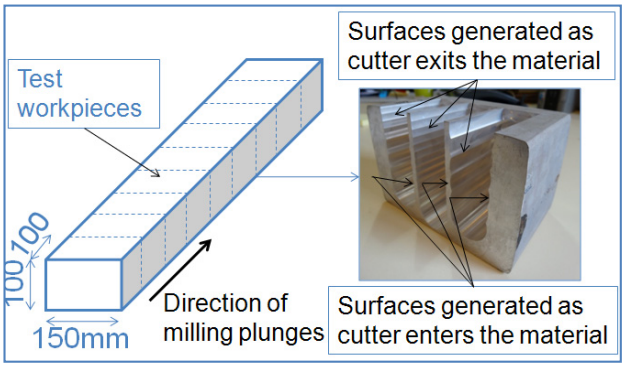


Fig. 1. Taking sample test coupons from forged bars and direction of plunge milling.

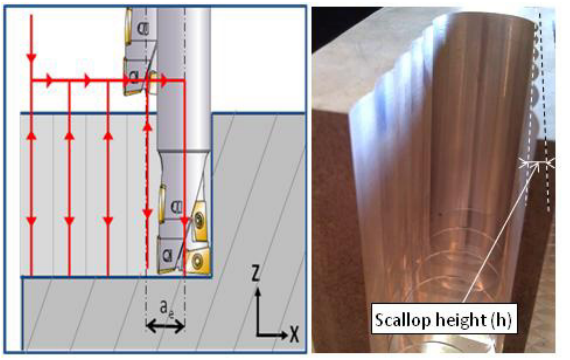


Fig. 2. Plunge milling operation parameters.

## 2.1. Chip flow in plunge-milling

On each plunge, the milling cutter is offset by a value ae determining the surface of material removed, in the form of a lunula (Fig. 3). The chip removal rate Qc is computed from the area of the lunula and the feed rate Vf. In the present instance, it was decided to stick to a cutting speed Vcmax=200% of Vc*, corresponding, using a 16.5 mm radius cutter, to a rotation speed just below 10000 rpm. Thus, the maximum chip removal rate is 2.279 dm3/min, which is reached with Vcmax, fzmax and ae2. With Vcmin, fzmin and ae1, the chip removal rate is 38 cm3/min.

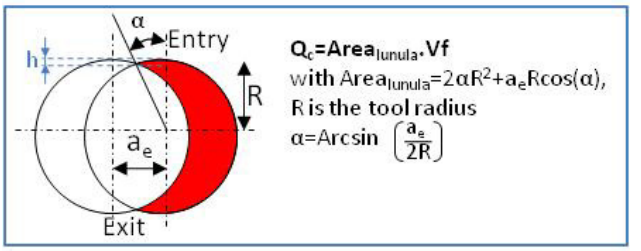


Fig. 3. Computing the chip removal rate Qc.

## 2.2. Observations and measurements

The study was intended to correlate the cutting parameters with surface characteristics such as the surface condition, its roughness, its microstructure or even also the residual stresses caused by machining. The milled surfaces were studied using an environmental Scanning Electron Microscope (SEM), as also by looking at images provided by a contact-free 3D roughnessmeter so as better to interpret the SEM images, especially for vibrations and pull-outs, or again for material bonding. Measurements with the 3D roughnessmeter were made on imprints from the milled surfaces taken with Plastiform DAV resin offering accuracy down to a micron. This means a reverse image of the surfaces is obtained, with a hollow in the 3D roughnessmeter image being in reality representative of extra material on the surface, while a peak will in fact correspond to a material pull-out (Fig. 4). These surface irregularities are not readily interpretable using an SEM alone. Roughness was measured with a Mahr Perthometer roughnessmeter, in accordance with standard ISO 4288.

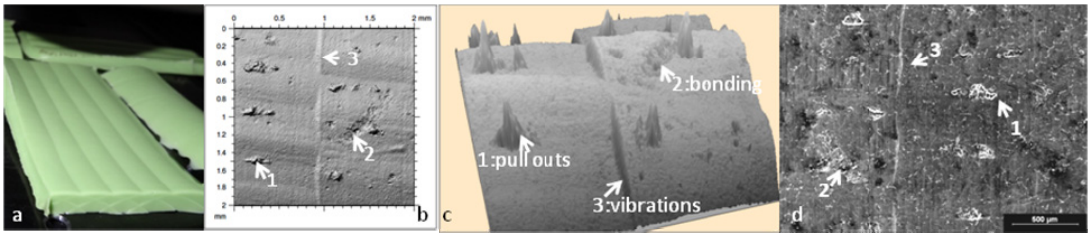


Fig. 4. a) Surface imprints; b) and c) Images of a surface given by the 3D roughnessmeter and types of defects; d) SEM image of the same surface and types of defects.

The microstructure was studied using an optical microscope, a SEM and a microhardness meter with a Vickers indenter and a 10gf load applied during 10s. Each plotted point at a given depth below the surface was averaged over three measurements. The machined surfaces were cut in accordance with Fig. 5 and polished, then chemically etched (Nital 10%) for instances of observations under the optical microscope.

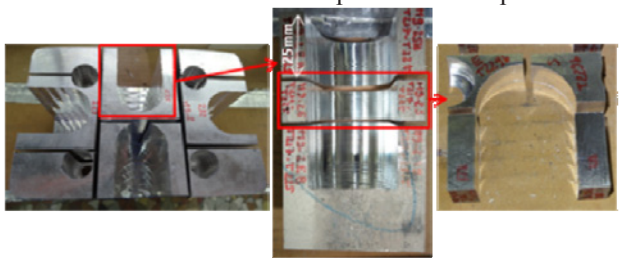

Fig. 5. Cutting out test coupons for observations. The figure on the right corresponds to the surface orthogonal to the direction of the cutter plunge. This is the surface studied in 3.3.

Residual stresses were measured using an X-ray diffractometer in accordance with the sin2ψ method. However, such measurements proved to be impossible to implement due to the presence of texture on the workpiece. Thus these results will not be presented here.

## 3. Results and discussion

### *3.1. Plunge-milled surface condition*

The plunge milled surfaces were observed under the SEM in order to determine the influence of the cutting parameters.

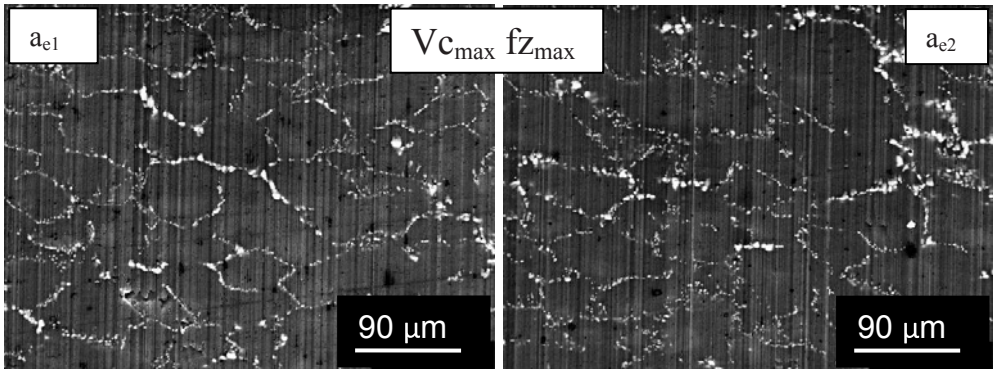


Fig. 6. Plunge milled surfaces with Vcmax, fz=max, and ae2 (a) or ae1 (b).

### *3.1.1. Influence of radial offset $a_e$*

At milling cutter entry and exit, observations show that the radial offset has no influence on the surface condition. At equal cutting speed and feed rate, the same surfaces are obtained taking ae1 or ae2 (Fig. 6).

### *3.1.2. Influence of the cutting speed Vc*

Different trends can be observed according to the values for feed fz, and according to whether the entry or exit of cutting is considered (Fig. 7, 1st and 2nd columns).

On entry as on exit, the surfaces do not show defects at fzmin, whatever the cutting speed.

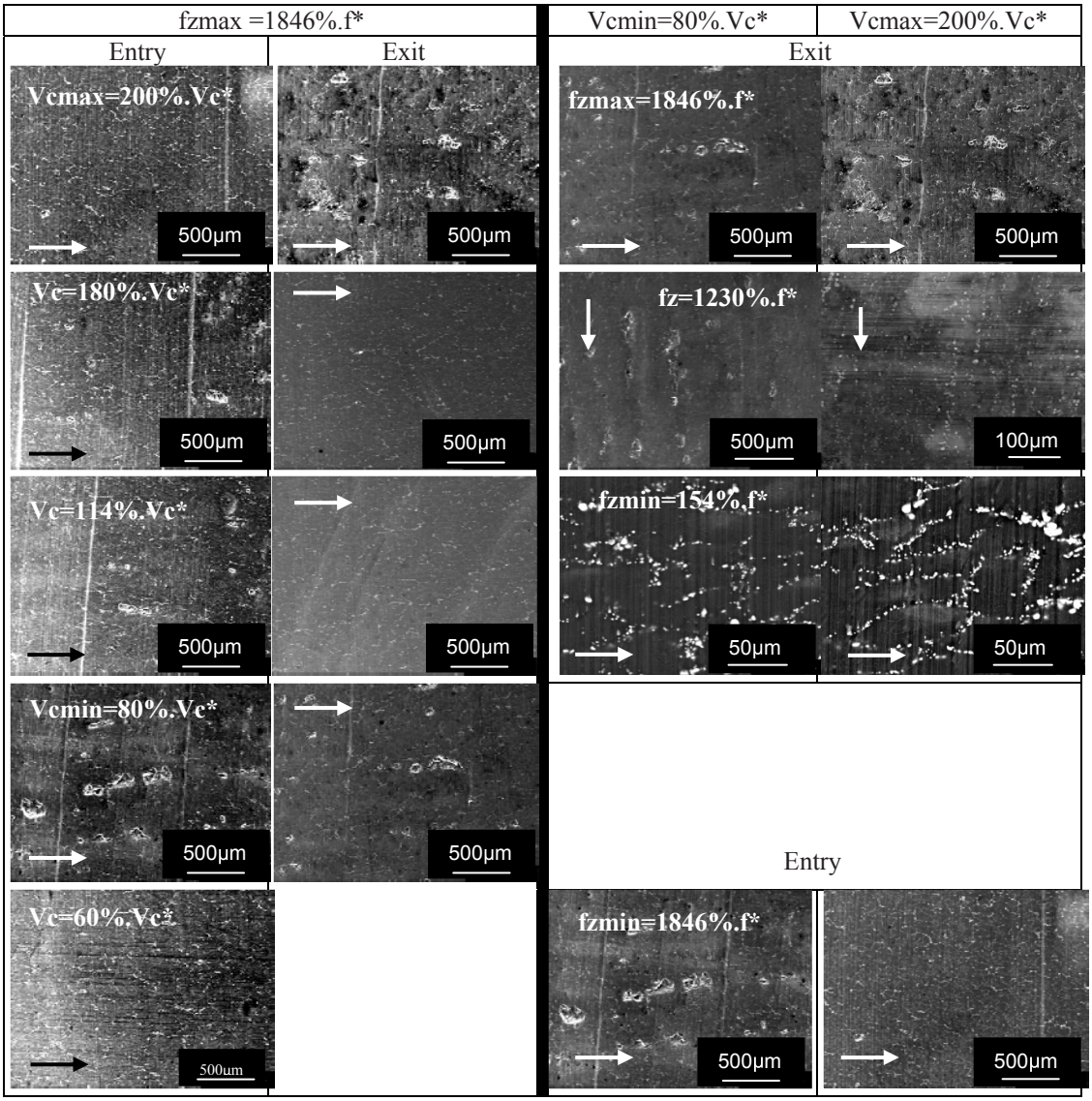


Fig. 7. Plunge milled surfaces: on the left, with fzmax on cutting entry and exit; on the right, with Vcmin and Vcmax on cutting exit and on entry for fzmax. On each picture, the arrow shows the milling cutter plunge direction.

However, at fzmax, a net improvement in the surface is observed when Vc increases from Vcmin to Vcmax, and the surfaces are also "clean" (without pull-outs of more than 10 μm nor vibrations visible on SEM) for Vc<Vcmin (3 tests were performed at Vc=60%.Vc*). Indeed, for a cutting speed between Vcmin=80%.Vc* and 180%.Vc*, pull-outs (of the order of 300 μm) and vibrations can be observed. On exit, the surfaces on the interior of the parameters domain are clean, while the surfaces obtained at the limits of Vc (at Vcmin and Vcmax) show pull-outs and vibrations. Again, at exit, with a feed of 1230%.f*, there is a "clean surface" at Vcmax, and a deteriorated surface at Vcmin.

*3.1.3. Influence of feed rate per tooth fz*

As for the cutting speed, a combined influence of Vc and fz can be seen, being different on entry and exit.

At Vcmax, a clean surface is obtained whatever fz on entry, while on exit fzmax gives a deteriorated surface condition. The setting should therefore be fz⩽1230%.f* to obtain a clean surface (Fig. 7, 1st image valid whatever fz on entry, and 4th column for exit).

At Vc=114%.Vc*, exit shows no defects whatever fz. On entry fzmax causes multiple pull-outs and vibrations, whereas the surface obtained at fzmin is clean.

At Vcmin, vibrations accompanied by pull-outs as from fz=1230%.f*, vibrations without pull-outs at fz=923%.f*, and a clean surface at fz⩽461%.f* are observed on entry and on exit (Fig. 7, 3rd column).

A combined influence of Vc and fz is thus seen, leading to different optimal conditions according to whether cutting entry or exit is considered. If the chosen machining strategy is to generate surfaces with the cutter entry, Vcmax and fzmax (and thus Qcmax) can be reached so as to obtain a surface without pull-outs, micro-cracks or vibrations. If, conversely, the resulting surface is produced on cutting exit, either the cutting speed (Vc=180%.Vc*) or the feed rate (fz=1230%.f*) must be reduced slightly to obtain a clean surface. As the chip removal rate is of greater interest in the first case, fzmax and Vc=180%.Vc* will be the most appropriate choice.

As the radial offset has no influence, the choice can be made in relation to the maximum scallop height sought on the walls.

It can be seen as a general rule that there is very little bonding deposit left on the plunge milled surfaces. This is certainly due to the cutting tools chosen that have an extremely sharp edge of just a few microns and a polished rake face that helps the chips slide smoothly.

It can be seen that the pull-outs are always parallel to the vibrations and seem to follow the same frequency (more visible on Fig. 4.b). In the literature, the forced vibrations due to cutting are explained as resulting from periodic variations in forces, cutter off-centring, or non-uniformity of the material (Moreau). In our case, these vibrations neither relate to the cutting forces nor the thickness of the chips, given that they are observed under different cutting conditions giving widely varying levels of loads. Similarly, a non-uniform microstructure is present here, and the fact that plunge cuts are made in a zone with elongated grains or a zone with equiaxial grains in no way changes the surface obtained. In a single case, these vibrations were not accompanied by pull-outs. For the same rotational speed, different surfaces were observed on entry and exit, showing that sounding of the assembly or of the cutter did not enable zones of vibrations related to an eigen-frequency, for example, to be avoided.

These surfaces can be validated despite the presence of the force measurement plate, thanks to comparisons of tests with and without the plate and also through using the high-speed camera (40 images/s) that shows that it is the milling cutter that vibrates and not the assembly. Those phenomena could depend on the kind of tool-holder attachment: HSK attachment is indeed known to be more rigid than the ISO40 type for instance.

It can also be noticed that low Vc always causes vibrations and defects such as pull-outs when combined with high feed rate (from fz=1230%.f*). Moreover, the entry strategy permits to use the maximum cutting conditions (Vcmax, fzmax and aemax) without obtaining vibrations, pull-outs or bonding deposits. So this strategy must be verified according to other parameters, such as geometrical ones, or regarding fatigue life. If those parameters present good results too, production users will be able to always use the maximum chip removal rate, allowing important reductions in costs.

For some tests, servos traces of the machine tool were recorded with a Siemens 840D CNC controller, a measuring system internal to the numerical control permitting the recording of the feed rate for instance. They could explain why the surfaces performed at low Vc and high fz present more pull-outs, bonding deposits and vibrations. Indeed, it can be observed that the feed rate control loop allows important gaps, so that the axis keeps accelerating and slowing down. These gaps are more important in the case of low Vc and high fz, causing more movement interferences with the theoretical trajectory. Nevertheless, that does not explain why the surfaces look worse at the tool exit than at the tool entry.

### *3.2. Roughness*

In the tests conducted, where the cutter moves up against the material it has machined, the insert may take up material again as it rises, as shown in the tests filmed using the high-speed camera. The basic roughness is then modified. The fact as to whether the cutter re-machines or not as it comes out of the material appears to relate to the level of the cutting forces, given that this does not occur in the weakest cutting conditions (Fig. 8).

Apart from feed per tooth fz, it remains difficult to correlate the cutting conditions directly with roughness values. However, roughness always increases with the feed rate. A level can be noted below which the surfaces are clean (without visible pull-outs nor vibrations), and above which the surfaces show vibrations and pull-outs of material. This level will be different according to whether cutting entry or exit is considered. The degree of roughness seems to be less on exit than on entry. This may be due to the tool rising up and taking material with it mostly on cutting exit.

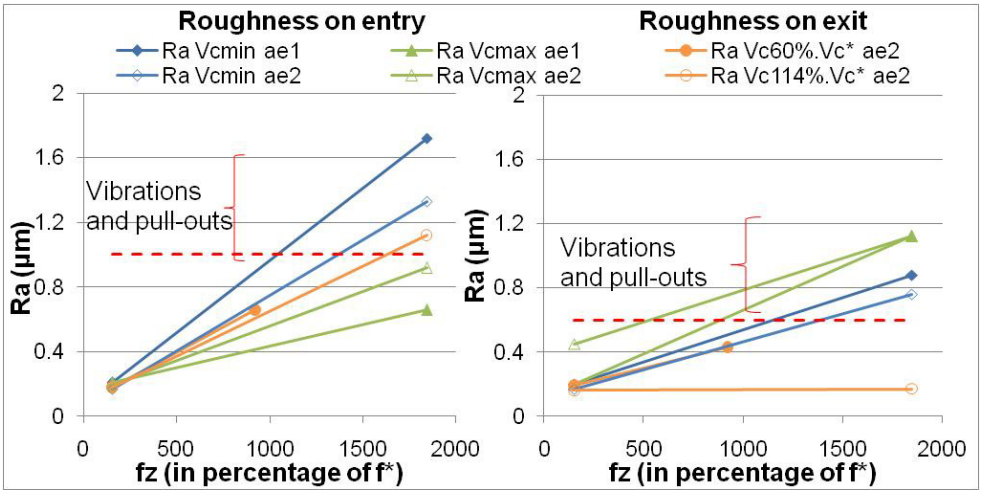


Fig. 8. Roughness in relation to feed on cutting entry and exit. In both cases, the surfaces are clean below the dotted red line, but above it they show pull-outs and vibrations. In the legend, Ra Vcmin ae1 corresponds to tests at Vc=Vcmin and ae=ae1.

### *3.3. Microstructure*

#### *3.3.1. Grain orientation*

The figure 9 shows the surfaces obtained at the extreme limits of the design of experiments, as well as the material at 3 and 6 mm under the surface. A change in orientation of the grains between the two cutting conditions can be seen, but the same change takes place at depth under the surface, showing that the non-uniformity is due to forging or other processes used to obtain the rough bar, and not to machining. No layer comparable to that found by Pu et al was present.

Indeed, Pu et al revealed a major change in the crystalline structure on the machined surfaces during orthogonal cutting, with Vc=100 m/min and fz=0.1 mm/th. They obtained a layer of ten microns in thickness where the grains

had in fact become nano-grains, thus changing the surface properties. This was due to the type of tool, with unpolished rake face and 30 to 70 µm edge radius (instead of a few microns in the present case). Moreover, even if the current study looks like orthogonal cutting regarding the horizontal cutting edge, the studied surface is the wall left by the vertical cutting edge of the insert (Fig. 2), so this seems normal that no layer comparable to that found by Pu et al was observed in the present study. Bhowmick et al also observed a grain boundary displacement in the drilling direction in a cast magnesium alloy, with HSS drills. This displacement seems to be related to the cutting temperature as it differs if using lubrication or not. In the present case, no change in structure was seen to take place under any of the conditions tested, which shows that there is no increase of temperature, certainly due to sharp cutting edge and polished rake face.

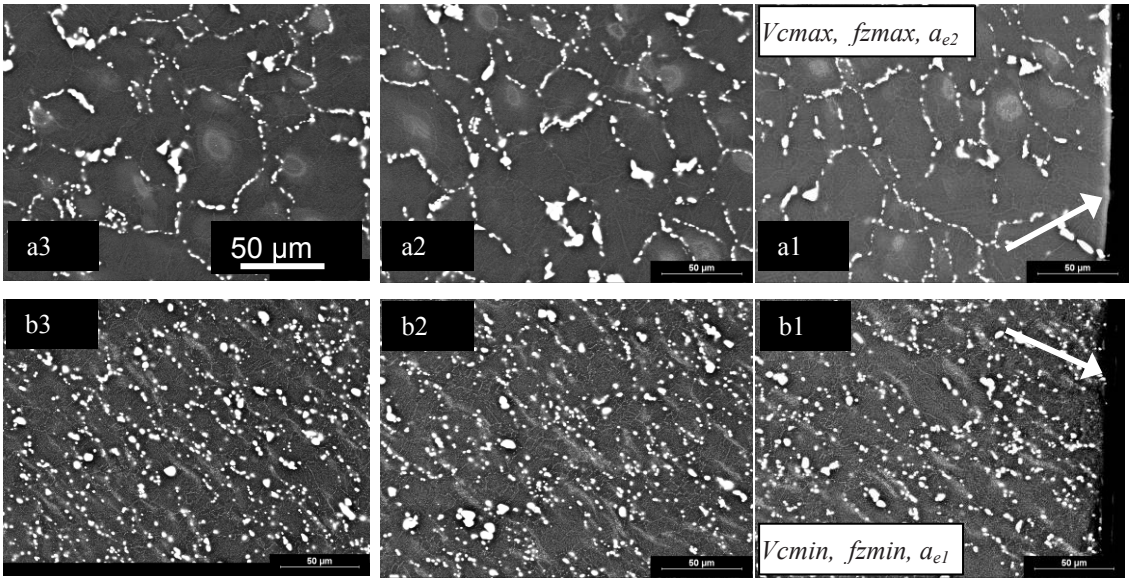


Fig. 9. Microstructure on the surface (a1 and b1), at 3 mm under the surface (a2 and b2), and at 6 mm under the surface (a3 and b3).

### 3.3.2. Microhardness

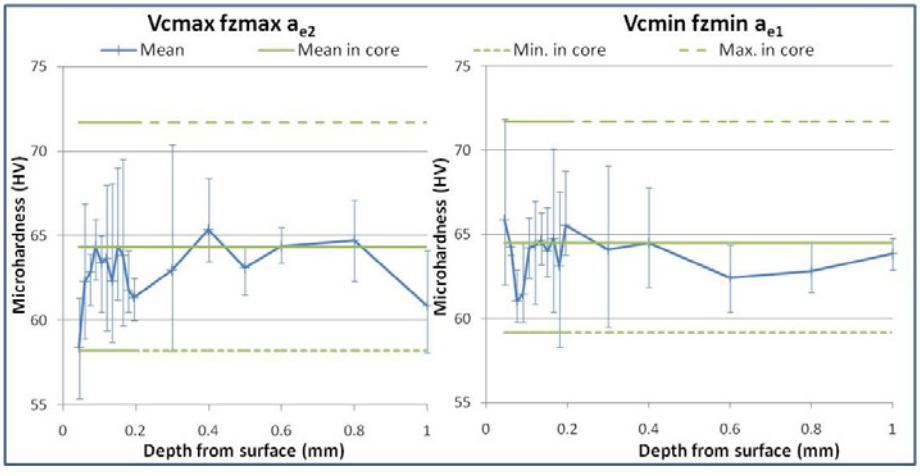


Fig. 10. Mean microhardness measured from the surface down to 1 mm under the surface.

Microhardness measurements (Fig. 10) tend to converge with the above results, meaning that machining has no influence on the microstructure. In both the extreme cases, hardness measurements on the surface remain within the range of hardness values found in the core (that is about 5mm under the surface). However, in the case of maximal cutting conditions, a light softening can be observed on the first 100 μm below the surface. Bhowmick et al revealed a notable softening in the case of dry drilling of a cast magnesium alloy with HSS drill, until 300 μm below the surface (from 35 kg.mm-2 just below the surface to 52 kg.mm-2 at 350 μm). The difference of results can be explained by the quality of tool (uncoated carbide with sharp cutting edge and polished rake face).

## 4. Conclusion

The present study shows that the surfaces obtained in plunge milling and their quality depend on the conditions and the machining strategy. It seems more interesting to generate the resulting surface from the milling cutter entering the material, as this strategy allows the more important cutting conditions while also limiting vibrations and pull-outs of material. However, this remains to confirm regarding other parameters (dimensional criteria, fatigue life, or type of tool attachment). As the radial offset has no influence, it can be chosen according to the desired scallop height.

The cutting conditions have shown no influence on the microstructure in terms of plastic deformation at the grain boundary or microhardness, so it will be possible to use the maximal cutting conditions.

Finally, measurements of residual stresses proved impossible to perform on wrought Elektron 21 due to its texture. Checking the influence of machining on the texture of the material should be the subject for further works.

## Acknowledgements

The authors would like to thank Philippe DARNIS of the I2M Laboratory at the University of Bordeaux, for his assistance and for having enabled them to use the laboratory's contact-free 3D roughnessmeter. The authors would also like to thank the CARAIBE project, which is supported by national funds (FUI) and the AEROSPACE VALLEY cluster.

## References

Altintas Y., Ko J.H., 2006. Chatter stability of plunge milling in CIRP annals, Manufacturing Technologies 55, Issue 1, 361–364.

Bhowmick S., Lukitsch M. J., Alpas A. T., 2010. Dry and minimum quantity lubrication drilling of cast magnesium alloy (AM60). International Journal of Machine Tools & Manufacture 50, 444-457.

Kielbus A., 2007. Microstructure and mechanical properties of Elektron 21 alloy after heat treatment, Journal of Achievements in Materials and Manufacturing Engineering 20, 127–130.

Ko J.H., Altintas Y., 2007. Time domain model of plunge milling operation. International Journal of Machine Tools & Manufacture 47, 1351-1361.

Lyon P., Syed I. andHeaney S., 2007. Elektron 21 – an aerospace magnesium alloy for sand cast and investment cast applicationry. Advanced Engineering Materials, 9, 793-798.

Moreau V., 2010. Etude dynamique de l'usinage et de l'interaction pièce-outil par mesure des déplacements: application au fraisage et au tournage. Thèse de l'ENSAM.

Pu Z., Outeiro J.C., Batista A.C., Dillon Jr O.W., Puleo D.A., Jawahir I.S., 2012. Enhanced surface integrity of AZ31B Mg alloy by cryogenic machining towards improved functional performance of machined components. International Journal of Machine Tools & Manufacture 56, 17-27.

Salahshoor M. and Guo Y.B, 2011. Surface integrity of biodegradable orthopaedic magnesium-calcium alloy by high-speed dry face milling. Production Engineering, 5, 641-650.

Wakaoka S. et al., 2002. High-speed and high-accuracy plunge cutting for vertical walls. Journal of Materials Processing Technology 127, 246–250.

Witty M. et al., 2012. Cutting tool geometry for plunge milling – Process Optimization for stainless steel. 5th CIRP conference on high performance cutting.